INSIGHTS INTO ULTRASONIC WELDING OF ABS-PC (MYCHRIL) POLYMERS: CHARACTERIZATION AND PERFORMANCE ANALYSIS

R. Sharanabasavaraj, S. Arungalai Vendan*, M. Chaturvedi

Department of Electronics and Communication, School of Engineering,
Dayananda Sagar University, Bengaluru, India
*Corresponding author's e-mail address: arungalaisv@yahoo.co.in

ABSTRACT

This study looks at the characterization and performance of ultrasonic welding for ABS-PC (Mychril) polymer blends used in EV station applications. Experiments were conducted and a detailed characterization of the welded interfaces were performed using Scanning Electron Microscopy (SEM) to examine their structure. Fourier Transform Infrared Spectroscopy (FTIR) was deployed to identify chemical interactions and any potential degradation, and X-ray Diffraction (XRD) to evaluate changes in crystallinity caused by the welding process. SEM images showed consistent fusion and minimal voids, while FTIR and XRD tests showed that key functional groups remained intact with slight changes in crystallinity. Mechanical tests were also carried out on the welded samples that involved tensile, impact and fracture assessments. Pearson's heat map coefficient analysis was performed to understand the influence of input process parameters on the mechanical strength outcomes. This research shows that ultrasonic welding is a suitable, sustainable, and effective method for assembling ABS-PC samples in EV applications, providing mechanical reliability and design flexibility.

KEYWORDS: mychril, ABS, PC, ultrasonic welding, SEM, FTIR, Pearson correlation, heatmap

1. INTRODUCTION

The rapid expansion of electric vehicles (EV) is driving the demand for electric vehicle infrastructure requiring lightweight, durable and low-cost materials generally used in essential charging station attributes. Acrylonitrile Butadiene Styrene ABS-Polycarbonate ((PC)-Mychril grade) polymer blends are common materials used in these applications since it has excellent impact resistance, dimensional stability and electrical insulation.

The traditional methods used to join polymer blends, specifically ABS-PC, has limitations in strength, accuracy and speed of production. Ultrasonic welding (USW) is a solid-state joining process that provides opportunity to quickly, cleanly and efficiently join these polymers without the need for adhesives or fasteners.

The research will examine the characterization and operational performance of ABS-PC welds with ultrasonic welding. The main methodologies will be SEM, FTIR, and XRD to characterize and analyze the structural integrity, chemical stability and crystallinity of the welds. The results will inform and support the establishment of reliable and viable implements for future manufacturing EV station components using USW. Ultrasonic welding has emerged as a viable option in a wide range of industries such as aerospace electronics automotive and particularly for connections between dissimilar materials, such as metals and polymers [1-4].

Ultrasonic welding is performed by applying ultrasonic vibrations to the joints of materials without adhesives, bolts, or soldering materials. Ultrasonic welding utilizes mechanically generated vibrations in ultrasonic frequencies (20kHz to 70kHz) to generate heat from indirect and direct friction and fuse the materials at their interface. Ultrasonic welding creates joints with high force precision, strong joints, and less distortion [5-7]. Authors investigated ultrasonic welding of ABS plastic and 5052 aluminium in the context of EV light weighting [8].

The experimental and simulation results indicated that the joint strength peaked at 17.87MPa, corresponding with a welding time of 1700ms, after which it declined due to thermal degradation of the ABS. Authors also reported the formation of the ABS weld using ultrasonic that occurs in five phases, including melting of the polymer and its subsequent

Date of submission/acceptance: 27.09.2025/15.12.2025
https://doi.org/10.35219/awet.2025.05

collapse and residue formation, all of which impacted joint integrity and failure mode [8].

In the study by Feistauer et al. [9], hybrid joints were created by ultrasonically welding textured titanium and aluminium alloy (Ti-6Al-4V) to glass fibre reinforced polyetherimide (GF-PEI) using the u-joining method. The paper illustrates the usage of Box–Behnken experimental for parameter optimization and producing stronger joints. The authors stated the maximum shear strength (3608 ± 417 N) and the minimum lack of penetration (0.10 ± 0.05 mm), when welding energy values of 2012.1 J, welding pressure of 14.7 psi, and oscillation amplitude of 52 μm were used.

Lionetto, Balle and Maffezzoli [10] studied the USW process to join carbon fiber reinforced epoxy resin composites to aluminium foil sheets (AA5754) while integrating a polyamide 6 (PA6) film to reduce the limitations caused by thermoset resins at high temperatures. The average adhesion (34.8 MPa) was obtained through the optimization of welding energy and force, with a morphological study identifying that direct contact was obtained or that the in contact lay carbon fiber inserted into aluminium. Authors investigated the friction stir welding (FSW) processes of PA66 utilizing an induction-heated tool and a strip of PA66-GF30 as reinforcement, with the aim of improving joint performance. The optimal conditions (1000 RPM, 20 mm/min) achieved a homogeneous dispersion of fibres and a stability in material flow at 91% joint efficiency, while over-heating was shown to cause fibre agglomeration and to degrade them. The findings of this research show the importance of keeping heat input in check, and reinforcing the materials for a higher quality polymer FSW joint [11]. PC/ABS formulations are used a great deal, due to their good mechanical properties; ultrasonic welding is a favourable method of joining. Thermal analysis (DSC, TG) data showed limited change to glass transition temperature and onset temperature after welding with any degradation in samples primarily associated with the ABS component. SEM observations of PC/ABS blends provided evidence of the structural integrity of the weld joint, and the variation in activation energy profile suggested that in blends with higher PC content had more complex degradation mechanisms. Many studies have investigated the ultrasonic welding of thermoplastics as well as experimental studies, mechanical testing and material quantification studies.

There is also a number of studies with regard to simulations, which is understandable because many of these studies are addressing similar problems. However, there is a very limited amount of research regarding the ultrasonic welding of ABS and PC (Mychril) blends specifically for samples used in electric vehicle (EV) applications. Ultrasonically welded PC-ABS is widely being explored in EV components owing to its excellent energy absorption, higher dimensional stability, and swiftness in weldability [12].

The blend aid in accomplishing a strong, repeatable and precise joints for interior panels, battery housings, sensor enclosures, and lightweight structural parts. Its superior stiffness–toughness characteristics make it ideal for thermally stable and vibration resistant EV assemblies [13].

Ultrasonic weld joint quality and efficiency depend on controlled parameters such as frequency, amplitude, weld time, and holding time along with the geometry of the energy director. This study integrates experiments, simulations, and image-processing analysis to show the influence of these factors on the heat generation, defect detection and weld integrity thereby offering insights for designing advanced ultrasonic welding systems [14].

A comprehensive overview of ultrasonic welding, detailing its key components and the material-specific benefits and challenges across metals and composites were also discussed by authors [15]. It also highlights critical weld-quality factors and optimization strategies, making it a valuable reference for applying ultrasonic welding in modern manufacturing. There are also research findings pertaining to the use of hybrid ERVFL-GBO AI model that accurately predicts ultrasonic welding behaviour in ABS-PC blends using experimental data from L27-based trials. The model outperforms other ERVFL variants in all statistical evaluations, demonstrating superior accuracy in estimating temperature and joint strength [16].

2. EXPERIMENTAL WORK

Polymer-welding techniques differ based on the physics underlying the heat generation and its transfer profile. Ultrasonic welding is swift and precisely delivers energy especially for complex smaller components. Whereas the vibration welding is appropriate for larger parts but produces more noise and flash. Hot-plate welding yields strong, hermetic joints, however, has longer heating and cooling times. The laser welding facilitates clean, particulate-free seams, nevertheless it requires laser-absorbing materials.

Based on these observations, ultrasonic welding is found to be appropriate and is thus chosen for this study. The methodology adopted in this study is illustrated as a flowchart in figure 1.

The experimental work for reliable, accurate and quick joining of EV power station Panel at UltraTech sonic Solutions, Basavangudi, Bangalore was carried out. A conventional ultrasonic welding machine consists of a number of basic components. The components of the ultrasonic welding machine include transducer, booster, sonotrode (or horn), and anvil.

The transducer is the converts electrical energy into mechanical vibrations. The booster intensifies the vibrations and transmits them to sonotrode, that Similarly applies the transfer of the vibrations to the workpieces that bond them under pressure in figure 2.

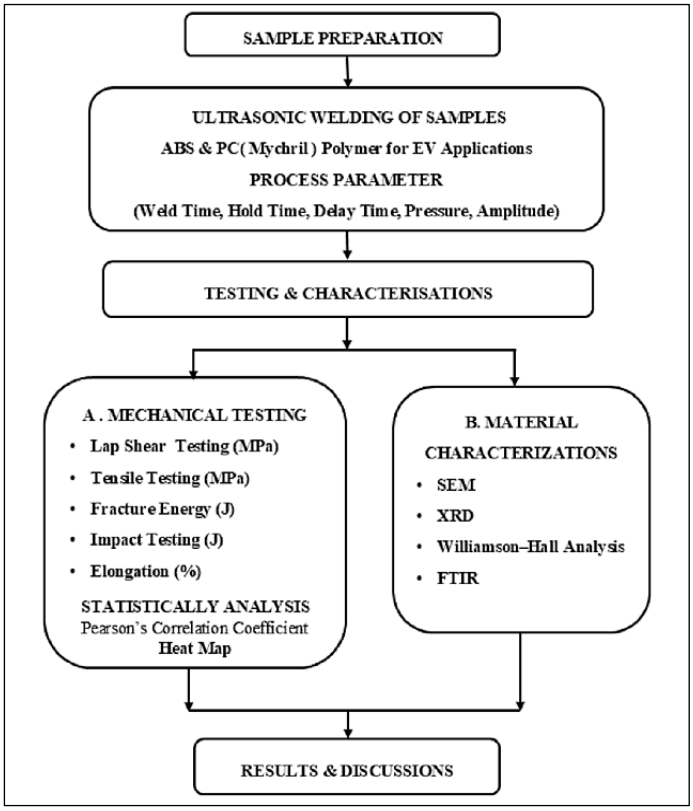

Fig. 1. Research methodology

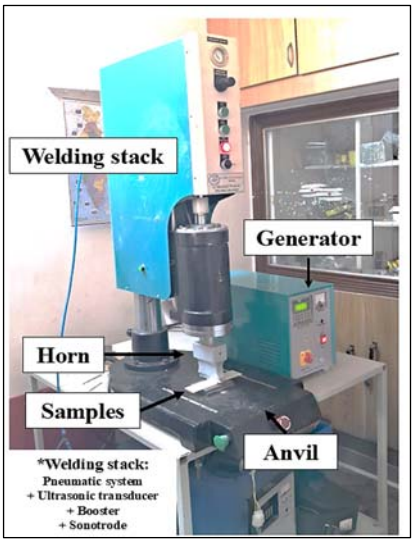

Fig. 2. Ultrasonic welding equipment

The ultrasonic welding system consists of several key components, including a power generation subsystem in figure 2, which is designed to provide high-frequency excitation from a standard single-phase 50 Hz electrical source through a power converter circuit. This power converter modulates and rectifies the standard input voltage, resulting in a high-frequency AC signal suitable for ultrasonic applications. The ultrasonic signal is then sent to the piezoelectric transducer, which converts the electrical energy into high-frequency mechanical oscillations. The oscillations are subsequently amplified by an amplitude booster to enhance the vibrational displacement for effective energy transfer. The amplified mechanical energy is delivered to the workpieces by the ultrasonic horn (or sonotrode), which is designed at a geometry specifically for any particular component geometry to provide an optimum vibrational couple and ensure consistent weld quality for high-volume parts production. The table 1 lists the characteristics of the ultrasonic weld machine.

Table 1. Characteristics of the ultrasonic welding equipment

Operating frequency [kHz]	Maximum force [N]	Weight of equipment [Kg]	Weld generator-max. power output [W]	Weight of horn [Kg]
20	3000	115	900/2000/3000	6Kg

This paper presents experimentation undertaken on the ultrasonic welding process as an investigation in order to weld the different components of an electric bicycle panel - the parts of the panel include the transparent window shield, of PC (Mychril), ABS main frame component, and various brackets of PC component. In this study, the ultrasonic welding of these samples will involve lap welding of incompatible materials (ABS & PC), the change or variation in weld strength at vibrational frequency of 25kHz with three control parameters: static clamp pressure, weld time, delay time, hold time, amperage & power inputs (Table 2). The working range of the parameters was taken from the previous experimental work of Ultrasonic welding on various materials with different geometries of the samples [17]. Increasing the strength of polymer welds utilizes a number of methods; optimizing welding parameters, improving material properties, design considerations, post-processing methods etc. The work reported in this paper and the results show the optimized process parameters for welding. The experimentation involved joining 27 samples based on design of experiments by varying each of the input process parameters in 3 levels.

The weld samples shown in figure 3, having 3-4 mm thickness, were subjected to several tests and studies to determine how process parameters affect the weld. The simulation circuits were analysed to meet the objectives and the observations made are described in the following section.

Table 2. Process parameters. Experimental values for electric vehicle (EV) power station panel

Sample	WT [s]	HT [s]	DT [s]	P [Bar]	Power [W]	A [mA]	Sample Status
1	2.8	1.5	0.7	4	4	0.6	Welded
2	1.5	0.5	0.5	4	3	0.8	Welded

WT: Weld Time; HT: Holding Time; WT: Delay Time; P: Pressure, A: Amplitude.

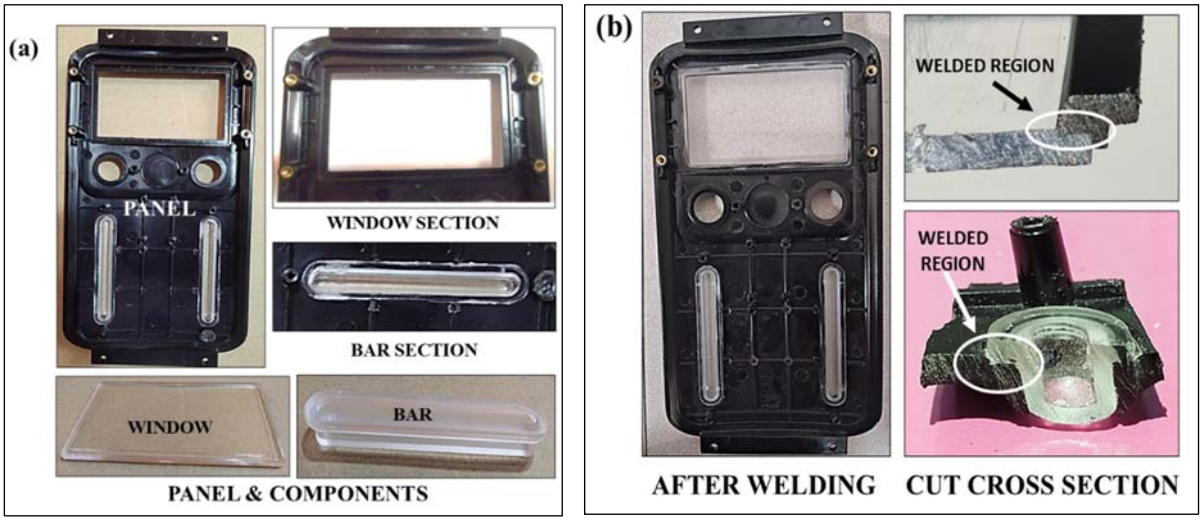

Fig. 3. The weld samples: a) weld specimen for the electric vehicle (EV) power station panel; b) cut cross section for SEM characterization

3. RESULTS AND DISCUSSION

3.1. SEM Analysis

The morphology of the welded joints created through ultrasonic welding of ABS-PC (Mychril) polymers was investigated using a scanning electron microscope (SEM). Hitachi 3400S Japan model instrument was used for microstructure analysis of Base ABS and PC (Mychril). It was also used for the welded combination of ABS and PC.

Based on the SEM micrographs of the weld interface and the following major findings were observed: When optimized welding parameters were employed, the interface showed a uniform and continuous fusion zone with little voids or defects, which indicated good molecular interdiffusion and bonding between the ABS and the PC phases.

An apparent heat-affected zone was also recorded directly adjacent to the weld line indicating localized melting and flow of polymeric chains. There were neither signs of thermal degradation nor excessive burn-off material found at the optimized parameters.

These findings fortify the role of ultrasonic welding parameters have an effect on the microstructure of ABS-PC joints in succession to the welds' mechanical performance shown in figure 4.

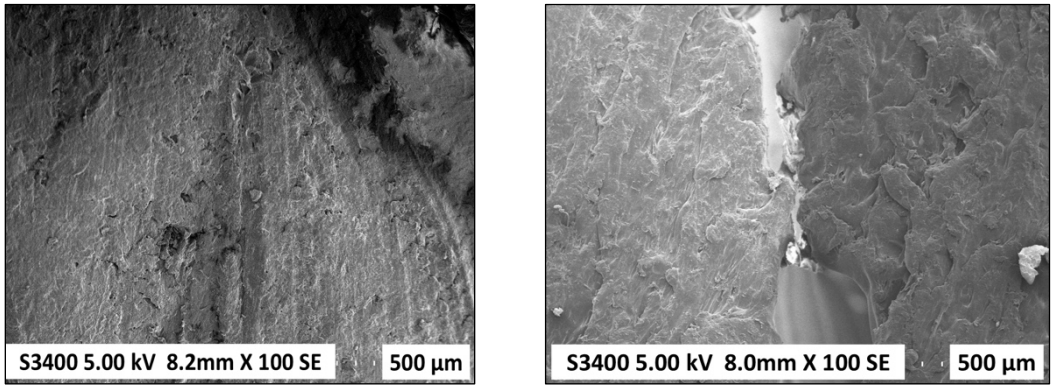

Fig. 4. SEM image of welded ABS-PC polymer

3.2. X-ray Diffraction Analysis

X-ray Diffraction (XRD) analysis was performed to assess the crystallinity and phase changes in ABS-PC (Mychril) polymers before and after ultrasonic welding. The base ABS-PC (Mychril) polymer showed mainly an amorphous structure, characterized by broad diffraction halos and a lack of sharp crystalline peaks in figure 5. This pattern is typical for thermoplastic polymer blends.

After ultrasonic welding, the XRD patterns did not show any significant shift in the characteristic amorphous halo, indicating that the overall crystalline nature of the material stayed mostly the same. However, a slight increase in peak intensity around 2θ (17° to 22°) suggests that there was some minor orientation or densification of polymer chains at the weld interface. This change likely resulted from the localized heating and pressure during welding. No new peaks corresponding to additional crystalline phases were found, which confirms that ultrasonic welding does not cause chemical breakdown or phase changes in ABS-PC under the given conditions.

Minor changes in the full width at half maximum (FWHM) of the amorphous hump indicate slight relaxation and reorganization of polymer chains. This could enhance interfacial bonding without affecting the overall amorphous nature.

These observations confirm that ultrasonic welding mainly leads to localized chain movement and densification rather than crystallization, helping maintain the functional and dimensional stability of ABS-PC.

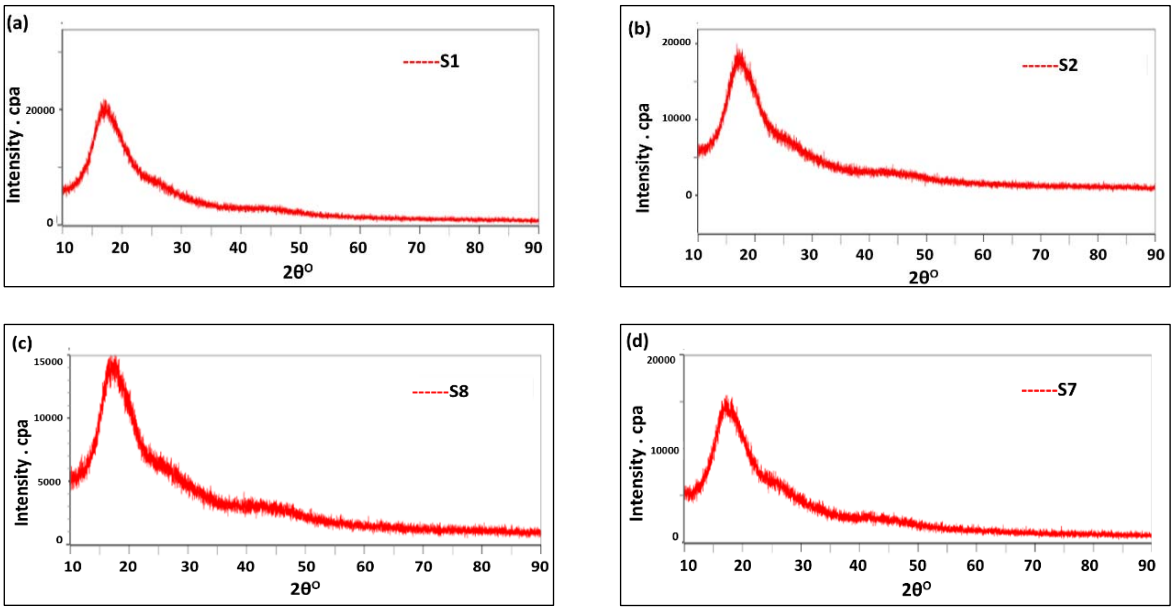

Fig. 5. X-ray Diffraction Pattern: a) base PC; b) base ABS; c) ABS-PC window; d) ABS-PC bar

3.3. Williamson–Hall Analysis

Williamson–Hall (W–H) analysis was performed to estimate the crystallite size and lattice strain of the ABS-PC (Mychril) polymer before and after ultrasonic welding. The W–H plots are generated by plotting βcosθ against 4sinθ, where β is the full width at half maximum (FWHM) of the diffraction peak, and θ is the

Bragg angle in figure 6. The W–H plot for the base ABS-PC polymer was approximately linear and demonstrated the amorphous form with very small or negligible amount of crystalline part. The resulting crystallite size was already large (>100 nm) and also suggested low structural order with very low lattice strain. This is expected due to the polymer being an amorphous thermoplastic blend. The welded sample displayed some broadening in the peaks, suggesting the introduction of localized strain and some microstructural reorganization at the weld interface. W–H analysis trial agreed well by demonstrating a small reduction in crystallite size and corresponding increase in lattice strain, which could result from high frequency mechanical vibrations and localized heating during the welding process. Although the sample continues to behave as an amorphous polymer and does not appear to show considerable crystalline or new phase emergence, the lattice strain likely remains low enough to allow for additional chain entanglement and inter-diffusion, thereby improving weld strength without altering the bulk material's properties. These outcomes support the findings of SEM and XRD, demonstrating that ultrasonic welding only modifies localized structural features without causing degradation or crystallization. The comparative summary of W-H analysis for different samples is provided in table 3.

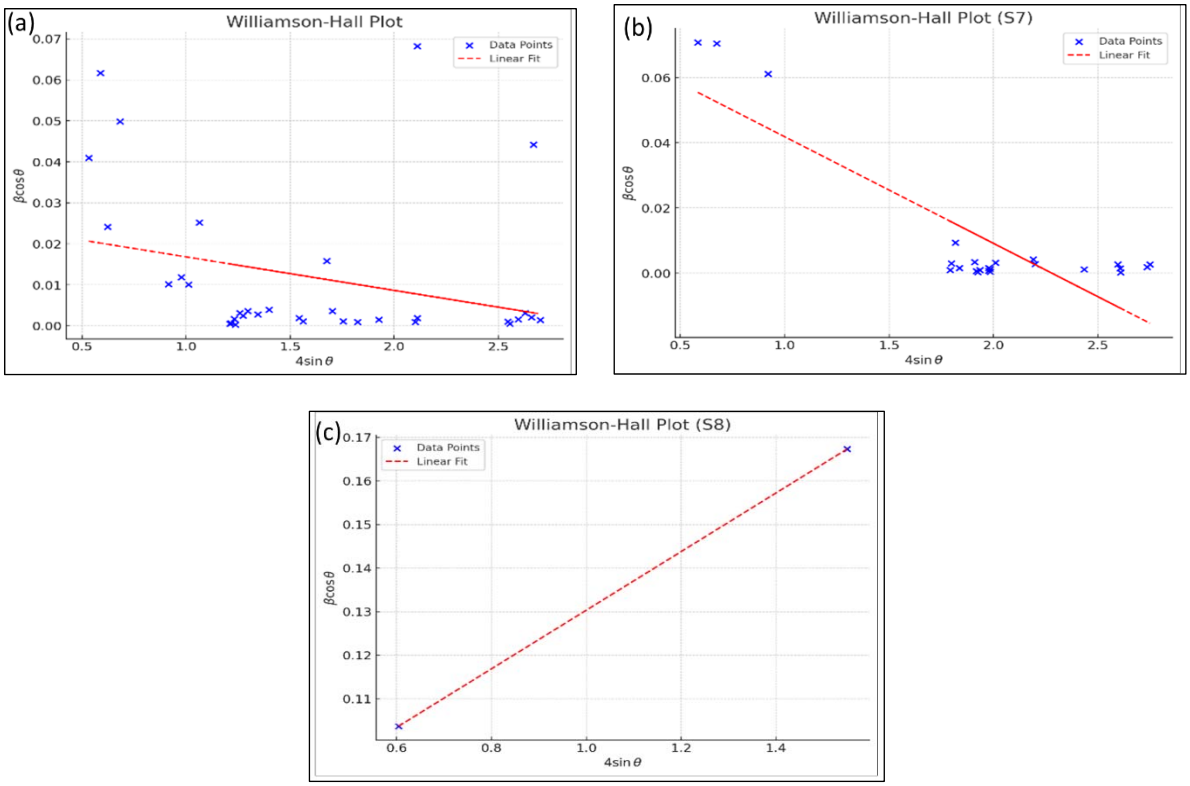

Fig. 6. W-H plot of: a) base material PC; b) welded ABS-PC (window); c) welded ABS-PC (bar)

Table 3. Comparative summary of Williamson-Hall (W-H) analysis for S1, S7, and S8

Sample	Crystallite size (DDD)	Micro strain [ϵ]	Strain type
S1	55.48 nm	0.00817 (0.82%)	Compressive
S7	18.59 nm	0.0327 (3.27%)	Compressive
S8	21.99 nm	0.0673 (6.73%)	Tensile

3.4. Fourier Transform Infrared Analysis

FTIR spectroscopy (Fourier Transform Infrared Spectroscopy) was used to examine functional groups and assess any potential chemical changes in the ABS-PC (Mychril) polymer before and after ultrasonic welding. The FTIR spectrum of the base ABS-PC showed characteristic absorption bands for its samples:

- C≡N stretching (nitrile group of ABS) at ~2235cm^{-1}.
- C=O stretching (carbonate group in PC) at ~1775cm^{-1}.
- C=C stretching (aromatic rings) at ~1600cm^{-1}.
- C–H stretching of aliphatic chains at ~2920cm^{-1} and ~2850cm^{-1}.
- C–O–C stretching (carbonate linkage) at ~1220cm^{-1}.

These peaks provide confirmation of the presence of functional groups of ABS (Acrylonitrile-Butadiene-Styrene) and PC (Polycarbonate) in the polymer blend. The FTIR spectrum of the welded joint displayed all major peaks of the characteristic peaks of ABS-PC, indicating that there were no substantial chemical degradation and no formation of new functional groups. Only small changes in the C=O stretching and C≡N stretching regions were observed, likely due to localized heating and pressure during the welding process leading to some minor chain orientation, intermolecular interactions, and rearrangement of the atomic structures of the polymer blends.

There were no new peaks, confirming that ultrasonic treatments do not lead to oxidation or degradation of the polymer structure, in figure 7. The similarities of the FTIR spectra demonstrate the chemical stability of the ABS-PC during ultrasonic welding.

The intensity variations observed demonstrate localized rearrangements at the weld interface that correspond to enhanced mechanical interlocking, without altering the chemical composition.

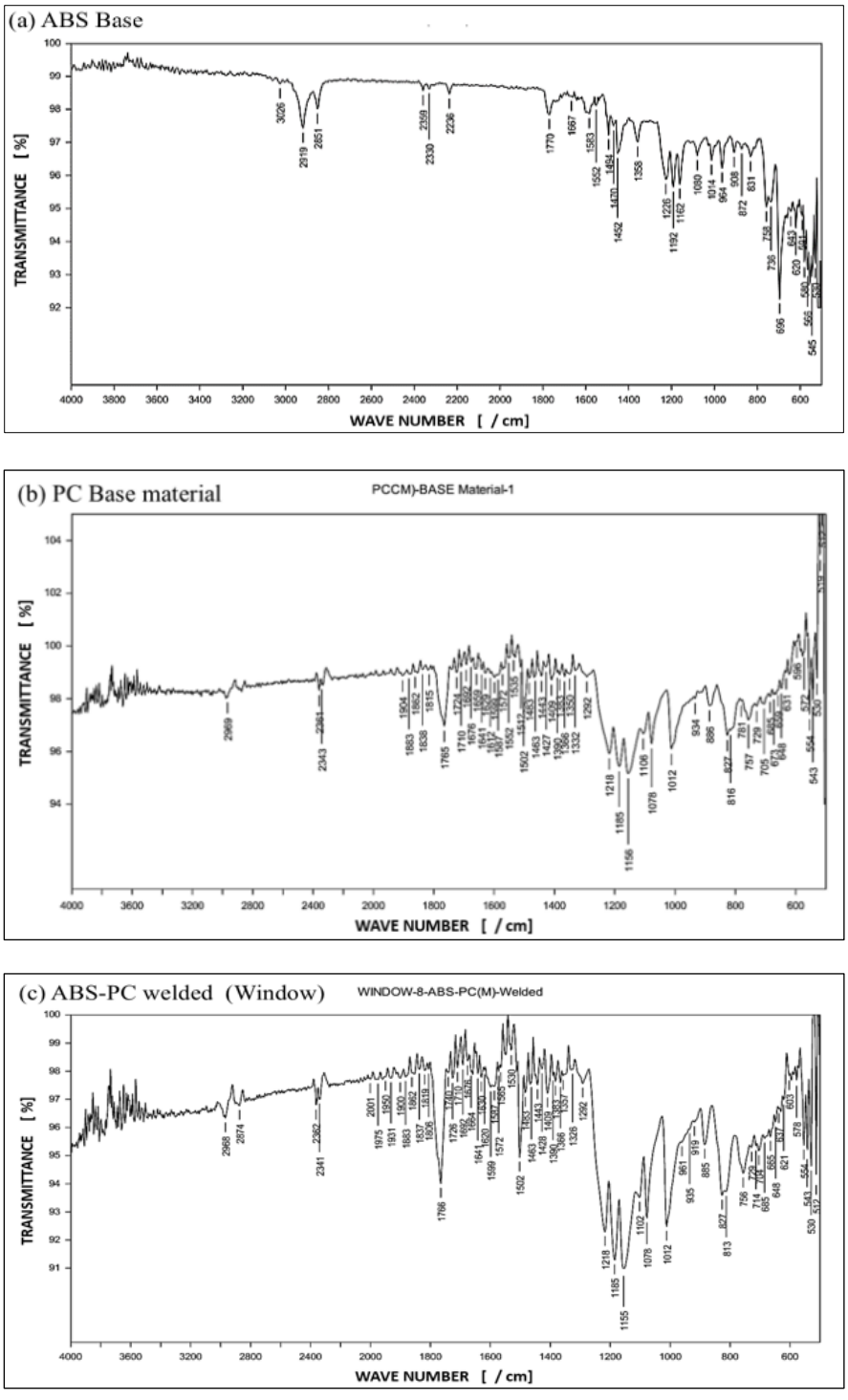

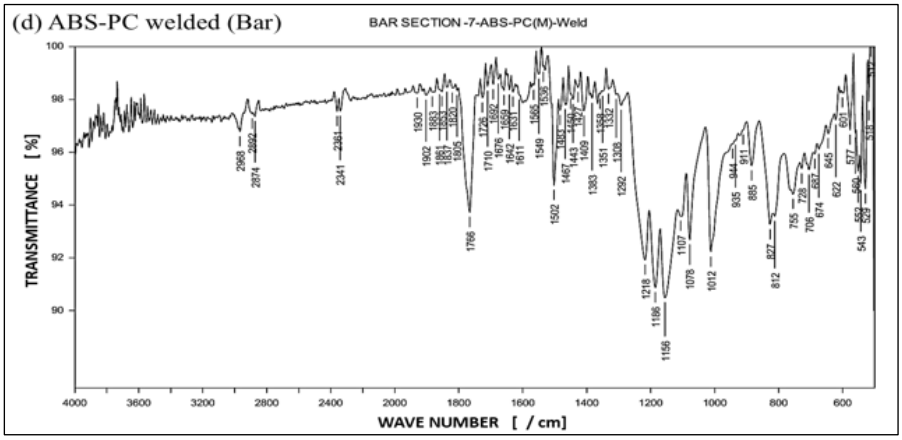

Fig. 7. FTIR Analysis: a) base material ABS; b) base material PC; c) welded ABS-PC (window); d) welded ABS-PC (bar)

3.5. Mechanical Testing

Mechanical testing was performed on some of the weld samples to assess the impact of variation of process parameters on the tensile strength, lap shear, elongation, fracture energy, and impact capacity of the weld region.

Weld trials were made with a range of process parameters, decided based on the design of experiments. Three parameters, viz. Hold time, weld time, and vibration amplitude were controlled in three levels, and combinations of these values were used as the experimental trials for causing the weld in the samples. In table 4, experimental process parameters & mechanical testing results are listed. It is observed that the mechanical testing exhibits the required performance for optimal combination of process parameters.

Parameters of significance for all mechanical testing parameters were further analysed using Pearson's correlation coefficient.

3.6. Pearson Correlation

Pearson's correlation coefficient (r) is a popular statistic used to measure the degree of correlation between linearly related variables.

Researchers apply the point-biserial correlation using the Pearson correlation formula when one of the variables is dichotomous. The Pearson correlation coefficient r is computed using the formula (1):

$$r = \frac{\sum(x_i - \bar{x})(y_i - \bar{y})}{\sqrt{\sum(x_i - \bar{x})^2}\ \sqrt{\sum(y_i - \bar{y})^2}} \quad (1)$$

where xi, y_i are individual data points
$\bar{x}$, $\bar{y}$ - mean values of X and Y
r ranges from 1 to +1.

Table 4. Experimental process parameters & mechanical testing results

Run	Amplitude [µm]	Weld time [s]	Hold time [ms]	Lap shear [MPa]	Tensile [MPa]	Elongation [%]	Fracture energy [J]	Impact strength [J/m]
1	20	0.4	100	18.481	25.626	5.799	3.299	21.059
2	20	0.4	200	18.673	25.398	5.676	3.277	23.174
3	20	0.4	300	20.04	27.534	5.22	3.039	25.223
4	20	0.8	100	18.651	24.774	5.157	3.725	22.645
5	20	0.8	200	19.826	25.991	5.458	3.467	24.412
6	20	0.8	300	19.888	26.829	4.759	3.654	25.698
7	20	1.2	100	18.239	24.739	5.161	4.146	21.552
8	20	1.2	200	19.251	25.025	4.899	3.92	22.283
9	20	1.2	300	20.092	26.693	4.944	3.89	24.143
10	30	0.4	100	20.942	27.454	6.182	3.939	22.5
11	30	0.4	200	22.105	28.176	5.642	3.177	25.974
12	30	0.4	300	22.679	29.068	5.907	3.172	26.444
13	30	0.8	100	21.475	27.05	5.806	3.991	22.877

Run	Amplitude [µm]	Weld time [s]	Hold time [ms]	Lap shear [MPa]	Tensile [MPa]	Elongation [%]	Fracture energy [J]	Impact strength [J/m]
14	30	0.8	200	22.426	28.445	5.428	3.938	24.294
15	30	0.8	300	22.461	28.463	5.432	3.53	26.422
16	30	1.2	100	21.228	26.183	5.401	4.676	22.558
17	30	1.2	200	22.218	27.812	4.691	4.148	25.599
18	30	1.2	300	22.048	29.137	5.333	4.151	26.674
19	40	0.4	100	22.675	28.68	6.486	3.765	24.376
20	40	0.4	200	24.07	28.828	6.28	3.933	25.363
21	40	0.4	300	24.564	30.107	5.563	3.442	28.803
22	40	0.8	100	23.739	28.868	5.847	4.228	23.438
23	40	0.8	200	24.568	30.074	5.418	4.208	26.366
24	40	0.8	300	25.758	30.164	5.681	3.937	27.866
25	40	1.2	100	24.196	29.326	4.945	4.654	22.854
26	40	1.2	200	24.523	30.056	5.323	4.308	25.949
27	40	1.2	300	24.58	31.463	5.187	4.354	29.219

Table 5. Correlation insights of Pearson's correlation with process parameters & mechanical testing results

Correlation coefficient [r]	Amplitude [µm]	Weld time [s]	Hold time [ms]	Lap shear [MPa]	Tensile [MPa]	Elongation [%]	Fracture energy [J]	Impact strength [J/m]
Amplitude [µm]	1.00	0.00	0.00	0.95	0.87	0.38	0.46	0.52
WeldTime [s]	0.00	1.00	0.00	0.04	-0.01	-0.71	0.75	-0.04
HoldTime [ms]	0.00	0.00	1.00	0.26	0.42	-0.28	-0.34	0.79
LapShear [MPa]	0.95	0.04	0.26	1.00	0.94	0.23	0.37	0.69
Tensile [MPa]	0.87	-0.01	0.42	0.94	1.00	0.19	0.24	0.79
Elongation [%]	0.38	-0.71	-0.28	0.23	0.19	1.00	-0.24	-0.04
Fracture Energy [J]	0.46	0.75	-0.34	0.37	0.24	-0.24	1.00	-0.09
Impact [J/m]	0.52	-0.04	0.79	0.69	0.79	-0.04	-0.09	1.00

3.6.1. Heat Map for all Process Parameters with Mechanical Test Parameters

Pearson correlation coefficients are computed between the process parameters and the mechanical testing results to generate the correlation matrix, heat map, in figure 8. Table 5 gives the correlation insights of Pearsons correlation with process parameters & mechanical testing parameters.

The heat map indicates:

1. **Amplitude** shows strong positive correlations with Lap Shear (0.95) and Tensile (0.87), indicating that increasing amplitude significantly enhances joint strength. It also has moderate positive correlations with Impact (0.52) and Fracture Energy (0.46).
2. **Weld Time** has a strong negative correlation with Elongation % (-0.71) and a strong positive correlation with Fracture Energy (0.75), suggesting that longer weld times reduce flexibility but increase energy absorption before fracture. It has minimal effect on Lap-Shear (0.04) and Tensile strength (-0.01).
3. **Hold Time** is moderately positively correlated with Impact (0.79) and Tensile strength (0.42), showing that longer hold times slightly improve joint toughness and strength.
4. **Mechanical properties inter-correlations**: Lap Shear and Tensile strength are highly correlated (0.94), indicating that factors improving one often improve the other. Impact also shows strong correlations with Tensile (0.79) and Hold Time (0.79).

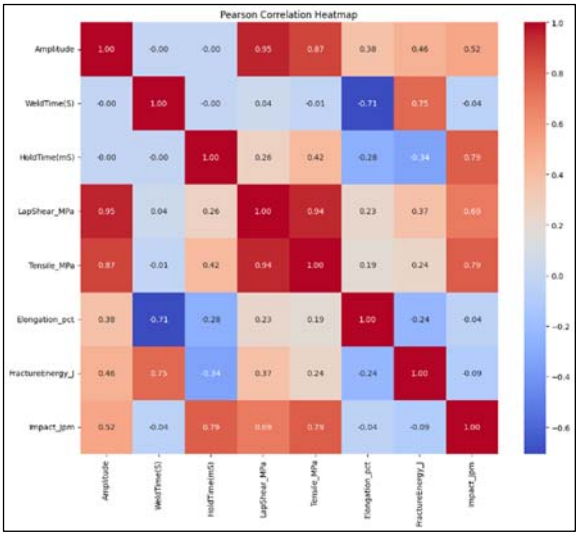

Fig. 8. Pearson correlation heat map for mechanical testing & process parameters

3.6.2. Heat Map for Process Parameters with Lap Shear Test

The Pearson correlation heatmap for the lap shear strength, in figure 9, shows the relationship between process parameters (Amplitude, Weld Time, Hold Time) and lap shear strength (LapShear_MPa).

The map indicates that Amplitude has a very strong positive correlation (0.95) with Lap Shear strength, meaning higher amplitude significantly improves joint strength. Hold Time shows a weak positive correlation (0.26) with Lap Shear, suggesting it has a minor influence on strength. On the other hand, Weld Time has almost no correlation (0.04) with Lap Shear, implying it does not strongly affect the strength in this dataset.

The process parameters do not show correlation with each other, indicating they act independently. Overall, amplitude is the most critical factor influencing lap shear performance, while hold time plays a secondary role, and weld time has negligible impact.

3.6.3. Heat Map for Process Parameters with Tensile Test

The Pearson correlation heatmap for the Tensile Strength, in figure 10, shows the relationship between process parameters (Amplitude, Weld Time, Hold Time) and tensile strength (Tensile MPa).

The map indicates strong positive correlation between amplitude & Tensile strength (0.87), making it the most influential process parameter for tensile strength. Hold time has a moderate positive effect (0.42), meaning longer hold duration moderately improves tensile strength.

Weld Time & tensile strength have negative correlation with (-0.01), indicating that the weld time has almost no effect on tensile strength. The process parameters show no correlation amongst themselves.

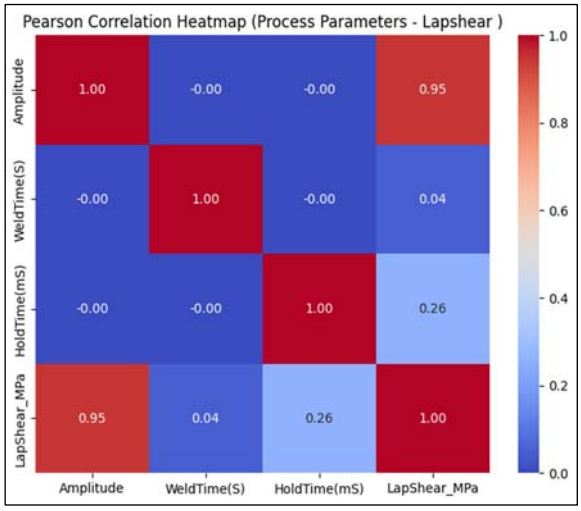

Fig. 9. Pearson correlation heat map for process parameters - Lap Shear Test

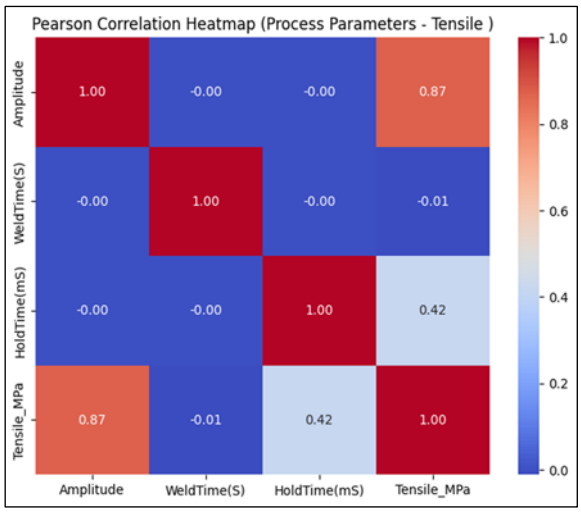

Fig. 10. Pearson correlation heat map for process parameters - Tensile Test

3.6.4. Heat map for Process Parameters with Elongation Test

The Pearson correlation heatmap for the Elongation test, in figure 11, shows the relationship between process parameters (Amplitude, Weld Time, Hold Time) and Elongation %.

The map indicates moderate Positive Correlation between amplitude & Elongation_% (0.38). Increasing amplitude moderately improves elongation percentage. Strong Negative Correlation is observed between Weld Time_ & Elongation_% (-0.71). Longer weld times significantly reduce elongation, indicating embrittlement due to over-welding. Weak Negative Correlation is noted between Hold Time & Elongation % (-0.28), suggesting that longer hold times slightly decrease elongation, but not as strongly as weld time. Negligible Correlation is indicated between the process parameters.

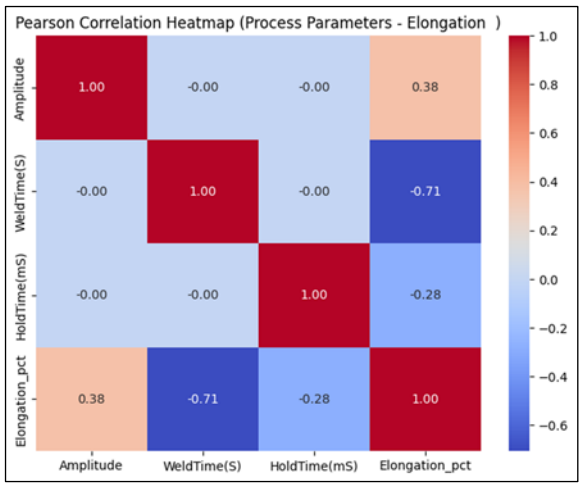

Fig. 11. Pearson correlation heat map for process parameters - Elongation test

3.6.5. Heat map for Process Parameters. Fracture Energy Test

The Pearson correlation heatmap for the Fracture energy test, in figure 12, shows the relationship between process parameters (Amplitude, Weld Time, Hold Time) and Fracture Energy.

The heat map indicates moderate positive correlation (0.46) between amplitude and fracture energy. Strong positive correlation (0.75) is observed between Weld time and fracture energy, indicating longer weld times improve bonding strength. Hold Time and Fracture Energy show moderate negative correlation (-0.34), suggesting that increasing hold time slightly reduces fracture energy.

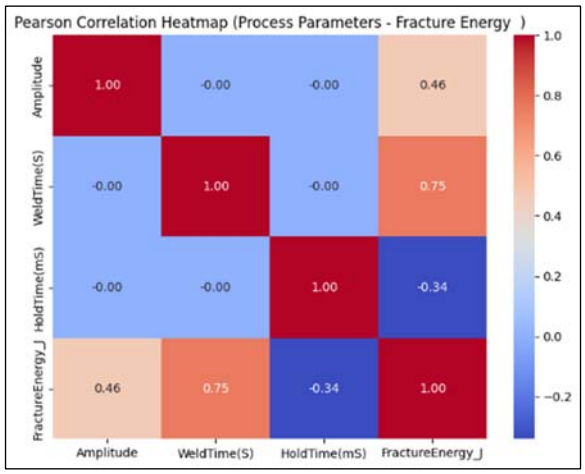

Fig. 12. Pearson correlation heat map for process parameters - Fracture Energy test

3.6.6. Heat Map for Process Parameters. Impact Test

The Pearson correlation heatmap for the Impact test, in figure 13, shows the relationship between process parameters (Amplitude, Weld Time, Hold Time) and Impact handling capacity at the weld.

The heat map describes a strong Positive Correlation between Hold Time & Impact intensity (0.79): impact strength. This indicates that holding pressure after ultrasonic welding contributes to better energy absorption and toughness. Moderate Positive Correlation is observed between Amplitude & Impact capacity (0.52), suggesting better interfacial bonding with increased amplitude. Negligible correlation is observed between the process parameters, with values of -0.04, 0 and 0.

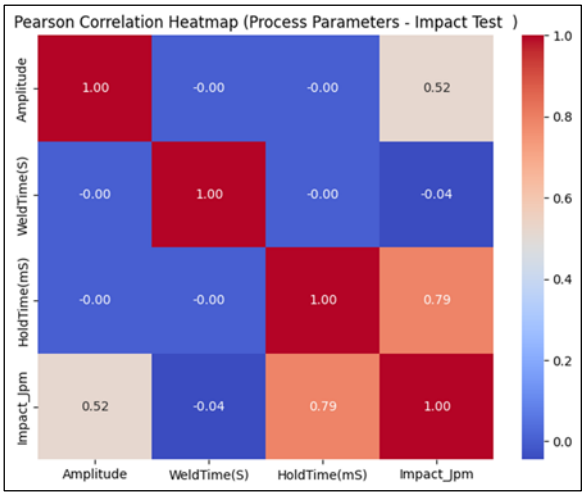

Fig. 13. Pearson correlation heat map for process parameters - Impact Test

4. CONCLUSIONS

Ultrasonic welding of ABS-PC (Mychril) polymers achieved solid and defect-free joints under optimised parametric range, proving appropriate for EV station component joining, based upon the appropriate tests conducted on the welded sample. The welded samples were tested and characterised for their microstructure, molecular arrangements, crystallinity, functional groups and dependencies of weld characteristics on the process parameters.

- SEM micrographs showed a homogeneous interface fused with little voids, showing effective molecular interdiffusion. Fracture surfaces presented many ductile features and brittle features indicating impact of variation in process parameters, apart from exhibiting effective energy absorption and good bonding.
- XRD test results indicated that the polymer blend remained amorphous after ultrasonic welding and little change in the peak intensity is suggestive only of reorientation of the chains and that ultrasonic welding caused no new crystalline phase to be formed.
- Williamson–Hall investigation confirms a slight decrease in crystallite size and increased lattice strain in the weld area, due to heat and pressure,

which would improve chain entanglement, without external affecting the properties of the bulk material.

- FTIR tests examined before and after the welding process indicated that all characteristic peaks of ABS-PC were present before and after welding with no new functional groups detected, thereby supporting the finding that ultrasonic welding does not cause any chemical degradation.
- Pressure deformation, as demonstrated by the decrease in intensity, indicated that no bulk structural change occurred, meaning that even though the intensity of the bond at the weld interface slightly overlapped, there was no change to the material integrity after welding.
- Pearson's correlation heatmap suggests that the Amplitude is the significant factor of influence for weld lap shear and tensile strength, Weld Time influences energy absorption and flexibility, and Hold Time contributes to toughness.
- Process optimization for weld strength should focus mainly on controlling amplitude and fine-tuning hold time. To preserve higher elongation (ductility), shorter weld times should be maintained, while longer weld time enhances fracture energy. For maximizing impact strength, hold time should be optimal with supportive tuning of amplitude.

The mechanical properties being strongly interrelated, reflect that optimizing one often affects others, and thus the results reported in this study will be significant in the selection of an optimal range of process parameters to obtain desired characteristics with the ultrasonic welding. The study emphasises that ultrasonic welding is a clean, efficient, and reliable process for joining of ABS-PC polymer, providing a feasible option for EV infrastructure possibilities. Besides, ultrasonic welding is cleaner, swift and more energy-efficient for polymer joining as compared to the vibration and laser welding, while still providing high joint strength with minimal heat-affected zones.

ACKNOWLEDGEMENTS

The authors would like to thank Mr. Alwin Raj Lobo & his team (Mr. Ravi & Mr. Dhanasekar), ULTRATECHSONIC Solutions, Bangalore for extending the facility & supporting us with technical guidance for carrying out this study.

REFERENCES

[1] **de Carvalho W. S., Draper J., Terrazas-Monje T., Toumpis A., Galloway A., Amancio-Filho S. T.**, *Fatigue life assessment and fracture mechanisms of additively manufactured metal-fiber reinforced thermoplastic hybrid structures produced via ultrasonic joining*, Journal of Materials Research and Technology, 2023, vol. 26, pp. 5716-5730.

[2] **de Carvalho W. S., Vacchi G. S., Rovere C. A. D., Amancio-Filho S. T.,** *Joining of additively manufactured fiber-reinforced thermoplastic and metals by ultrasonic energy: Mechanical and corrosion behavior*. Materials & Design, 2023, vol. 234, 112342.

[3] **De Leon M., Shin H S.,** *Review of the advancements in aluminum and copper ultrasonic welding in electric vehicles and superconductor applications.* Journal of Materials Processing Technology, 2022, vol. 307, 117691.

[4] **De Leon M., Shin H S.,** *Prediction of optimum welding parameters for weld-quality characterization in dissimilar ultrasonic-welded Al-to-Cu tabs for Li-ion batteries*. Metals and Materials International, 2023, vol. 29, pp. 1079-1094.

[5] **Unnikrishnan T G., Kavan P.,** *A review study in ultrasonic-welding of similar and dissimilar thermoplastic polymers and its composites.* Materials Today: Proceedings, vol. 2022, iss. 56, pp. 3294-3300.

[6] **Tilahun S., Vijayakumar M D., Ramesh Kannan C., Manivannan S., Vairamuthu J., Manoj Kumar K P.,** *A review on ultrasonic welding of various materials and their mechanical properties*. IOP Conference Series: Materials Science and Engineering, 2020, vol. 988, 012113.

[7] **Li H., Zhang C., Deng, Y., Zhou K., Ni Z., Yan F., Liu Q.,** *Interfacial reactions and joint performances of high-power ultrasonic welding of aluminum to steel.* Journal of Materials Research and Technology, 2023, vol. 26, pp. 328-343.

[8] **Tan X., Zhang S., Zhi Q., Li Y., Chen Y., Chen Y., Wen Z.,** *Characteristics and weld formation of ultrasonic welding of acrylonitrile butadiene styrene to laser-ablated aluminum alloy*, Optics & Laser Technology, 2025, vol. 192, 113442.

[9] **Feistauer E. E., Dos Santos J. F., Amancio-Filho S. T.,** *An investigation of the ultrasonic joining process parameters effect on the mechanical properties of metal-composite hybrid joints*, Welding in the World, 2020, vol. 64, pp. 1481-1495.

[10] **Lionetto F., Balle F., Maffezzoli.,** *A. Hybrid ultrasonic spot welding of aluminum to carbon fiber reinforced epoxy composites.* Journal of Materials Processing Technology, 2017, vol. 247, pp. 289-295.

[11] **Elsheikh A., Elmosalamy M., Ma N., Eldeeb, I., Showaib E., Ebied S.,** *Enhancing joint efficiency in friction stir welding of PA66 using an induction-heated threaded pin and glass fiber reinforcement*, Journal of Materials Research and Technology, 2025, vol. 37, pp. 4153-4164.

[12] **Chinnadurai T., Arungalai Vendan S.,** *Thermal and structural analysis of ultrasonic-welded PC/ABS blend for automobile applications.* Journal of Thermal Analysis and Calorimetry, 2017, 127, iss. 3, pp. 1995-2003.

[13] **Gupta P., Toksha B., Patel B., Rushiya Y., Das P. Rahaman M.,** *Recent developments and research avenues for polymers in electric vehicles*, The Chemical Record, 2022, vol. 22, iss. 11, e202200186.

[14] **Vendan Subbiah A., Chaturvedi M., Ka R. K., Radder S., Hammoodi K., Elsheikh A.,** *A synergistic approach to material analysis and power source engineering in ultrasonic welding of polymers*, Proceedings of the Institution of Mechanical Engineers, Part B: Journal of Engineering Manufacture, 2024, 09544054251318078.

[15] **Marxim Rahula Bharathi B., Singh A. K., Prasad D.V.S.S.S.V., Ramesh A., Elumalai P. V., Balaji N.S.,** *Ultrasonic Welding: Foundations, Influential Factors, and Material Applications*, Advanced Welding Technologies, 2025, pp.197-218.

[16] **Elsheikh A. H., Abd Elaziz M., Vendan,** *A modeling ultrasonic welding of polymers using an optimized artificial intelligence model using a gradient-based optimizer*, Welding in the World, 2022, vol. 66, iss. 1, pp. 27-44.